Evaluation of CV2025 ω-transaminase for the bioconversion of lignin breakdown products into value-added chemicals: synthesis of vanillylamine from vanillin[1]

C.J. Du, L. Rios-Solis, J.M. Ward, P. A. Dalby, G. J. Lye‡

[1]Department of Biochemical Engineering, University College London, Torrington Place, London, WC1E 7JE, UK.

Keywords: Lignin degradation; transaminase; bioconversion; vanillin; vanillylamine

1 Manuscript prepared for Biocatalysis and Biotransformation

‡Corresponding author (Email: g.lye@ucl.ac.uk)

ABSTRACT

Lignin is an essential component of the cell wall of various types of plants and represents an abundant and renewable natural resource. Both thermo-chemical and biological pre-treatment can be applied to break down the strong ether bonds and phenylpropanoid polymer subunits present in lignin. These liberate a range of phenolic compounds which represent potential substrates for bioconversion by ω-transaminases. In this work the use of CV2025 ω-transaminase (ω-TAm) from *Chromobacterium violaceum* DSM30191, heterologeously expressed in *E. coli* BL21 (DE3) Gold cells, is explored for selective amination of lignin breakdown intermediates into value-added products. Eight potential ω-TAm substrates were initially screened using (S)-α-methylbenzylamine (MBA) as the amino donor. Vanillin was identified as the best potential substrate which is converted into vanillylamine; an intermediate in the preparation of pelargonic acid vanillylamide used as a hyperemia inducing active substance in wound dressings. At low vanillin and MBA concentrations (<10mM) and with an excess of the amine donor (1:4 mol/mol) 100% w/w conversion of vanillin into vanillylamine was observed within 25 min. At vanillin concentrations above 10 mM, inhibition was observed decreasing the rate and yield of the bioconversion. The reaction product, vanillylamine and by-product (acetophenone) were also found to be inhibitory. Vanillylamine synthesis could be carried out by both whole cell and clarified lysate forms of the CV2025 ω-TAm while fed-batch bioconversions (feeding low concentrations of both vanillin and MBA) could help overcome substrate inhibition and double the final product concentrations obtained. These results demonstrate the potential for bioconversion of lignin breakdown products into value-added chemicals but illustrate the need for enzymes with improved substrate range and reduced sensitivity to product inhibition.

1. INTRODUCTION

Chemical and pharmaceutical companies are currently showing considerable interest in biocatalysis combined with the use of biorenewable feedstocks [1-4]. Compared to chemical syntheses biocatalytic routes to the same target compound can avoid the use of hazardous materials and organic solvents and generally require considerably less energy input [5]. For petrochemical derived synthons there are growing concerns over the stability and predictability of feedstock price [6, 7] which is raising interest in a shift towards biorenewable feedstocks.

Lignin is the most abundant aromatic substance present in the biosphere. It forms an irregular noncrystalline network in plant cell walls which is highly resistant to microbial degradation [8]. As a polymer it is composed of phenylpropanoid units linked through a variety of nonhydrolysable C-C and C-O-C bonds. It shows an inherent heterogeneity caused by variations in the polymer composition, size, cross-linking and functional groups [9]. Both biological and thermochemical methods exist for lignin pre-treatment and degradation [10-14]. From an environmental perspective biodegradation of lignin is advantageous as it is less energy intensive and potentially more selective [15-17]. However, both methods liberate a range of monomers that might represent useful starting materials for the synthesis of value-added chemicals [18, 19]. At present there are about 1.5 million tons of lignin-based products on the market including the food ingredient vanillin, and other breakdown products having applications in many fields such as the paper industry, synthetic resins, dyes, cosmetics, pharmaceuticals, regenerative energy source etc [20].

Aminated compounds are useful synthons in the manufacture of a wide range of fine chemicals and pharmaceuticals [21]. It is estimated that the majority of pharmaceuticals are synthesized from compounds possessing amine functionalities

[22, 23]. Amination, and ideally stereoselective amination, of lignin breakdown products is therefore an attractive option for increasing the value of the compounds liberated following thermochemical or biological pretreatment. Transaminases are ubiquitously present in microbes and higher organisms and have great potential for the production of natural and non-natural amino acids as well as chiral amines, which are in demand by the pharmaceutical industry [24-26]. The advantages of using transaminases over other enzymatic or chemical methods include high stereoselectivity and overcoming requirements for organic solvents or cofactor regeneration [27]. Transaminases are pyridoxal-phosphate coenzyme dependent catalyzing amino group transfer from a donor to the substrate of interest by a ping-pong bi–bi mechanism [28]. A wide range of amino donors have been reported in the literature one of the most common being (S)-α-methylbenzylamine (MBA) [29].

This paper explores the utility of the CV2025 ω-TAm from *Chromobacterium violaceum* DSM30191 for the selective bioconversion of a range of lignin breakdown products. The enzyme, previously cloned by us [27], is expressed in *Escherichia coli* BL21 (DE3) and can be used either as a clarified lysate or whole cell biocatalyst. It is shown that the CV2025 ω-TAm possesses good activity with a range of lignin breakdown products. From a commercial perspective the main limitations of the bioconversion appear to be substrate and product inhibition that currently limit the space-time yields that can be achieved.

2. MATERIALS AND METHODS

2.1 MATERIALS AND BIOCATALYST SOURCE

Nutrient broth and nutrient agar were obtained from Fisher Scientific (Leicestershire, UK). Competent *E. coli* BL21 (DE3) Gold cells were obtained from Stratagene (Amsterdam, NL). Vectors pQR800 and pQR801 were created in previous research [27]. Vanillin and benzaldehyde were purchased from Thermo Fisher Scientific (New

Jersey, US). All other reagents were obtained from Sigma-Aldrich (Gillingham, UK). All the reagents were of the highest purity available.

2.2 PLASMIDS pQR800 AND pQR801

Transaminase was expressed from plasmids pQR800 and pQR801 containing the complete *Chromobacterium violaceum* DSM30191 transaminase gene [27] in either native or His_6-tagged form respectively. These plasmids were constructed by using the expression vector $pET29(a)^+$ (5.3kb) which contains an inducible T7 promoter, the *lac* repressor sequence and codes for resistance to kanamycin. Plasmids were transformed into *E. coli* BL21 (DE3) Gold cells which were subsequently stored as glycerol stocks at -80°C.

2.3 CV2025 ω-TRANSAMINASE PREPARATION

E. coli BL21 (DE3) Gold cells containing the plasmid pQR801 were initially grown on LB glycerol agar plates (5 $g.L^{-1}$ yeast extract, 10 $g.L^{-1}$ Tryptone, 10 $g.L^{-1}$ NaCl, 10 $g.L^{-1}$ glycerol, 15 $g.L^{-1}$ agarose) containing 150 $\mu g.mL^{-1}$ kanamycin at 37˚C overnight. A single colony was then picked from the agar plate and cultured in a 250 mL shake flask with 20 mL of sterile LB-glycerol media containing 150 $\mu g.mL^{-1}$ kanamycin at 37˚C with orbital shaking at 250 rpm using an SI 50 orbital shaker (Stuart Scientific, Redhill, UK) for 11-16 hours. The entire contents of the 250 mL shake flask were then transferred to a 2 L shake flask with 180 mL of LB-glycerol media containing 150 $\mu g.mL^{-1}$ kanamycin, incubated at 37˚C, 250 rpm. When the OD_{600} reached between 1-1.5, isopropyl–β–D- thiogalactosidase (IPTG) was added to a final concentration of 0.1 mM. After 5 hours induction, glycerol stock could be produced by mixing 250 µL of cell suspension from the 2 L shake flask into 250 µL 20% v/v glycerol solution. This was stored in a 1.5 mL Eppendorf tube and kept in -80˚C freezer until use.

Cell lysate was prepared as follows: *E. coli* BL21 (DE3) Gold cells from shake flask cultures were harvested by centrifugation at 6000 rpm for 10 min in Falcon tubes. Following removal of the supernatant the cell pellet was resuspended in 50 mM

TRIS buffer containing 0.2 mM co-factor (pyridoxal-5-phosphate) at pH 7.5. This cell suspension was then sonication using a Soniprep 150 sonicator (MSE, Sanyo, Japan) with 10 cycles of 10 seconds, 10 μm pulses with 10s intervals on ice to avoid degradation of the enzyme. The sonicated suspension was then centrifuged again at 5000 rpm at 4˚C in an Eppendorf centrifuge for 5 min. The supernatant (soluble fraction, lysate) was filtered through a 0.2 μm filter to obtain clarified extract and either used immediately or frozen at -20˚C (control experiments showed no decrease in lysate CV2025 ω-TAm activity for over four months when stored in this way).

2.4 BIOCONVERSIONS

2.4.1 Screening for ω-TAm activity on lignin breakdown intermediates

Screening experiments were performed using an initial concentration of 20 mM of each potential substrate with 20 mM of the amino donor (S)-α-methylbenzylamine (MBA). The concentration of CV2025 ω-TAm clarified lysate used in the reactions was 0.3 $mg.mL^{-1}$, along with 0.2 mM of added PLP. Reactions were performed in a sealed 96-well glass microtiter plate to prevent evaporation with Nunc Aluminum Seal Tape (NY, USA) and incubated in an Eppendorf Thermomixer Comfort shaker (Cambridge, UK) for 24 hr. Reaction temperature was 30^{o}C and shaking was at 350 rpm (orbital shaking diameter 6 mm). 20 μL aliquots were taken at various intervals and rapidly quenched with 380 μL of a 0.2% v/v trifluoroacetic acid (TFA) solution. Samples were then centrifuged for 5 min at 13000 rpm and 300 μL of the liquid supernatant transferred to a HPLC vial for analysis.

2.4.2 Microwell scale bioconversions

A 96-well glass microtiter plate was used to perform small scale kinetic experiments. Random wells were first filled with amino donor solutions at final concentrations between 5 - 50 mM at pH 7.5 (from concentrated stock solutions). Next 0.3 $mg.mL^{-1}$ of either ω-TAm lysate or whole cell biocatalyst containing an equivalent quantity of enzyme, along with 0.2 mM of PLP, were added. The microtiter plate was covered with the Nunc Aluminum Seal Tape and then incubated at 30˚C for 20 min to

equilibrate all reaction components. To initiate the bioconversion the required substrate (amine acceptor) was added to the wells using an automatic multi-channel pipette (Research Pro, Eppendorf). This helped ensure all reactions could be initiated at the same time point which aids quantification of reaction kinetics and reproducibility. The reaction was incubated and shaken in a thermomixer for the desired period of time, 20 μL of sample were removed periodically for analysis.

2.4.3 Investigation of substrate and product inhibition

Experiments to examine substrate inhibition were performed varying the initial concentration of the desired substrate (or amine donor) between 5-50 mM while keeping the initial concentration of the amine donor (or substrate) fixed, typically at 5 mM or 20 mM. Experiments to examine product inhibition were performed at different added initial concentrations of product (or by-product) at the start of the bioconversion. Initial substrate concentrations were fixed at the desired level. All reactions were performed in a 96-well glass microtiter plate as described in Section 2.4.1.

2.4.4 Influence of biocatalyst form on stability

The stability of CV2025 ω-TAm activity in both lysate and whole cell forms was evaluated by incubation of the biocatalyst preparations for different lengths of time. Reactions were performed in a 96-well glass microtiter plate with each well initially containing 20 mM MBA, 5 mM vanillin and 0.2 mM PLP in 50 mM Tris buffer to a total volume of 300 μL. To initiate the bioconversion 50 μL of either lysate or whole cell CV2025 ω-TAm preparation was first added to the solution of reactants with shaking at 30^{o}C. Reactions were performed on a thermomixer at 30^{o}C, 350 rpm for 60 min with samples for HPLC analysis taken at specific time intervals. Other experimental conditions were as described in Section 2.4.1.

2.4.5 Comparison of lysate and whole cell ω-TAm activity

For a quantitative comparison of ω-TAm activity in either lysate or whole cell forms bioconversions were performed using identical concentrations of the CV2025 ω-TAm of 0.3 $mg.mL^{-1}$. Initial substrate concentrations were 40 mM MBA and 10 mM vanillin. All other experimental conditions were as described in Section 2.4.1.

2.4.6 Fed batch bioconversions

Fed-batch experiments were carried out in a 50 mL stirred glass reactor (with plastic cap) using 15 mL total reaction volume. Clarified lysate containing the CV2025 ω-TAm expressed from pQR801, was first incubated with 0.2 mM pyridoxal 5-phosphate in 50 mM TRIS buffer for 20 min at 30˚C. Speed was controlled using an IKAMAG RCT magnetic stirrer (Janke & Kunkel GMBH, Germany). Temperature was kept constant using a TXF200 Series heated circulating bath (Grant, UK). pH was maintained at pH 7.5 using a Metrohm 718 pH STAT Titrino and 806 Exchange Unit (Metrohm Ltd., Switzerland).

Experiments at low initial substrate concentration used 10 mM MBA and 5 mM vanillin, along with 0.3 $mg.mL^{-1}$ ω-TAm and 0.2 mM PLP. The feeds comprised concentrated solutions of MBA (170 mM, 0.88 mL) and vanillin (60 mM, 1.25 mL) pre-dissolved in the reaction medium. These were added following complete vanillin conversion at t = 1 hr and t = 2 hr in order to restore the initial starting concentrations of both substrates. Experiments at high initial substrate concentration used 60 mM MBA and 40 mM vanillin. The feeding commenced following complete vanillin conversion at t = 4 hr and t = 8 hr.

2.5 ANALYTICAL TECHNIQUES

2.5.1 Dry cell weight (DCW) measurement

1.5 mL aliquots of cell suspension were added to pre-weighed and dried 2.2 mL Eppendorf tubes, and then centrifuged at 13,000 rpm for 5 min (Eppendorf AG, Germany). The supernatant was discarded and the vials were left to dry at 90^{o}C until a

constant weight was achieved. The biomass concentration in $g_{DCW}.L^{-1}$ of the culture could then be calculated.

2.5.2 Optical density measurements for biomass quantification

Optical density measurements were performed at a wavelength of 600 nm (OD_{600}) using an Ultraspec 4000 variable wavelength spectrophotometer (Pharmacia Biotech, USA). A small aliquot of *E. coli* BL21 culture medium was taken from the shake flask cultures of the bioreactors and diluted with RO water so that the optical density measurement was between 0.1-0.8 absorbance units. The calibration relationship determined was that 1 OD_{600} unit was equal to 0.4 $g_{DCW}.L^{-1}$.

2.5.3 Protein quantification and SDS-PAGE analysis

Total protein concentrations were measured using Bradford reagent (Sigma-Aldrich), based on the method first described by Bradford [30]. Bovine serum albumin (BSA) was used as the standard for calibration curve preparation with absorbance being measured at 595 nm. SDS-PAGE analysis was carried out using a 12% resolving gel with a Tris-glycine buffer system stained with Coomassie Blue R-250 as described previously [31]. Approximately 20 µg of total protein was loaded into each well in order to make sure that the stained bands of background protein were still visible while the bands of overexpressed ω-TAm would not reach the saturation limit of the instrument. Labworks 4.5 analysis software from UVP (Cambridge, UK) was applied for the relative quantification of expressed ω-TAm in clarified enzyme lysates preparations based on density scanning of the gels.

2.5.4 HPLC analysis

A Dionex (Camberly, UK) microbore HPLC system controlled by Chromeleon client 6.80 software was employed for all RP-HPLC analyses. This system is comprised of a P680 gradient pump, ASI-100 automated sampler injector, STH 585 column oven and UVD170U UV detector. 4-hydroxy-3-methoxybenzaldehyde (vanillin), 4-hydroxy-3-methoxybenzylamine (vanillylamine), (S)-α-methylbenzylamine (MBA),

acetophenone (AP) and all other aromatic compounds (as described in Table I) were analysed on an ACE 5 C18 reverse phase column (150 mm x 4.6 mm, 5µm particle size; Advance Chromatography Technologies, Aberdeen, UK), using 0.1% v/v TFA at 1.0 mL min^{-1} with a gradient of acetonitrile from 15% to 72% over 9 min. The gradient was followed by 2 min of equilibration before injection of the next sample. The mobile phase flow rate was kept constant at 1mL.min^{-1} with solute elution measured at 275 nm. Quantification of solute concentrations was performed using calibration curves prepared with standards for each separate compound. The products were detected and quantified with respective to the peaks showing on the HPLC chromatograms at different retention time.

2.5.5 Purification of product

After the bioconversion, the reaction mixture was spun down (5000 rpm, at 4 °C for 15 min) and was then additionally filtered through a 0.2 μm sterile filter. 50 g of Amberlite IRA-410 resin (Sigma-Aldrich, Gillingham, UK) were added to the reaction mixture for 1 hr, and the resin was then removed by filtration. The remaining aqueous mixture was then passed through 80 g of an Isolute SCX-2 ion exchange column (Biotage, Uppsala, Sweden), and the column was washed with 400 mL of methanol. The column was then eluted with 500 mL 4 M NH_3 and the eluent was evaporated to yield the desired product.

2.5.6 Confirmation of product identity

Mass spectroscopy and Nuclear Magnetic Resonance (NMR) analyses were performed in the UCL Department of Chemistry. Chemical Ionisation (CI) mass spectrometry analyses were conducted on a Thermo Finnigan MAT900xp mass spectrometer. Methane was used as carrier gas. Operating conditions: capillary temperature 300°C, capillary voltage 9V, spray voltage 4.5 kV, sheath gas 80, auxiliary gas 30, and sweep gas 0 arbitrary units. Results are shown in additional information.

^{1}H NMR spectra were recorded on a Bruker ADVANCE III 600 (600 MHz) spectrometer, using D_2O solvent. The chemical shifts (δ) were given in ppm units relative to tetramethylsilane, and coupling constants (*J*) are measured in Hertz. Proton ^{1}H NMR multiplicities are shown as s (singlet), d (doublet), t (triplet), m (multiplet), dd (doublet of doublet), bs (broad singlet), bd (broad doublet), bt (broad triplet) and bm (broad multiplet). Results are shown in additional information.

3. RESULTS AND DISCUSSION

3.1 PRODUCTION OF TRANSAMINASE

E. coli BL21(DE3) GOLD cells transformed with plasmid pQR801, containing the CV2025 ω-TAm gene, were routinely grown in batch shake flask cultures as shown in Figure 1 (A). ω-TAm expression was induced with 0.1 mM IPTG when OD_{600} reached around 1 to 1.5. It can be seen that after adding IPTG at 3 hr, the growth of the transformed cells is retarded slightly in a way that is typical of cells overexpressing a heterologous protein [27]. The maximum biomass concentration reached was 1.4 $g_{DCW}.L^{-1}$ after 10 hours which was 18% lower than the untransformed cells.

In terms of the amount of ω-TAm produced analysis of the soluble protein fraction after cell lysis indicated a total protein concentration of 2.81 ± 0.03 $g.L^{-1}$ (error is 1 standard deviation about the mean from three replicate cultures). Figure 1 (B) shows an SDS-PAGE analysis of the soluble protein fraction from pQR801 expressing cells harvested at 8 hr. Lanes 2 and 3, from duplicate cultures, show over expression of ω-TAm at the expected molecular weight of 47 kDa [27]. Density scanning of the gels suggested that ω-TAm comprised 42 ± 4% w/w of total protein for the induced cultures. The specific yield of ω-TAm in the *E.coli* BL21-Gold (DE3) cells was therefore 0.2 $g.g_{DCW}^{-1}$ of cells. This level of expression is broadly in agreement with that found previously [27].

3.2 SCREENING OF ω-TAm ACTIVITY ON LIGNIN BREAKDOWN INTERMEDIATES

Several potential ω-TAm substrates were selected from both thermochemical breakdown and biodegradation pathways [32-34]. They were evaluated in order to explore the potential to synthesize value-added products via a bioconversion route. Screening reactions were performed at low initial substrate concentrations (≤ 20 mM) so as to minimize any substrate and/or product inhibition effects.

One of the issues with ω-transaminases is that they have a limited substrate range, with most accepting only substrates with a substituent no larger than a methyl group at the position adjacent to the ketone [35]. The results from Table I are in agreement with this hypothesis in that the smaller the group at this position the greater the activity detected. Vanillin showed the fastest initial reaction rate while conversions for substrates like acetovanillone and p-hydroxyacetophenone were very low due to the presence of the methyl substituent adjacent to the ketone. In these cases less than 10% w/w conversion could be reached in 24 hr. The last two compounds in the Table I did not react as expected since they do not posses ketone on aldehyde groups.

Since the focus of this work is to explore the use of ω-TAm for bioconversions to value-added chemicals vanillin was chosen for further study. Not only did it display the highest activity but it is known that the expected product, vanillylamine, can be readily converted into pelargonic acid vanillylamide used as a hyperemia inducing active substance in plasters [36]. Furthermore, work by Borrgaard Ltd. has shown that CO_2 emissions as a result of vanillin production from lignin are 90% lower than those for vanillin production from mineral oil derivatives [37].

3.3 VANILLIN BIOCONVERSION KINETICS

Having shown ω-TAm activity on vanillin, the next step was to examine in more detail the kinetics of the bioconversion using MBA as the amino donor (Figure 2 (A))

and to confirm the identity of the postulated vanillylamine product. Figure 3 shows the measured bioconversion kinetics determined at low equimolar substrate concentrations. The measured initial reaction rate was 1.1 $g.L^{-1}.hr^{-1}$ and a 79% w/w conversion was obtained in 12 hr. This suggests vanillin is a very good substrate for the CV2025 ω-TAm with both the rate and extent of conversion being higher than for many ω-TAm substrates previously investigated [27]. Confirmation of the identity of product made in preparative scale bioconversions (Section 3.2) was obtained by CI mass spectrometry (Section 2.5.6) and NMR spectroscopy (Section 2.5.6). The spectral fingerprints from these analyses can be found in Additional Information. These results confirm that the sample was indeed vanillylamine and that it was purified to a high standard.

3.3.1 Investigation of substrate and product inhibition

Commercial enzymatic synthesis of vanillylamine will need to be achieved with high substrate conversion and high product concentrations in order to be economically viable. Issues of substrate and product inhibition can often limit the rates and yields of ω-TAm bioconversions [38] and so these were investigated in further detail.

For bioconversions operated at a fixed MBA concentration of 20 mM, Figure 4 shows the influence of varying vanillin concentration on bioconversion rate and yield. At low vanillin concentration, quantitative conversion of vanillin into vanillylamine was obtained in under 30 min. However, at higher vanillin concentrations (> 10 mM) the bioconversion rate decreased due to increasing substrate inhibition. The impact of MBA concentration, as a typical amino donor used in ω-TAm reactions [29] was also evaluated at a fixed initial vanillin concentration of 5 mM. Figure 5 shows that no inhibition to the bioconversion was found for MBA concentrations up to 50 mM. In addition, once the ratio of MBA:vanillin concentration was over 2:1, the inhibitory influence of vanillin appeared to be reduced.

Achieving high product concentrations will be crucial for process economics and so

the influence of added vanillylamine on bioconversion kinetics was also studied with regard to product inhibition [39]. Since this experiment was performed at relatively high substrate concentrations, the reaction occurred over 24 hr. Based on Figure 6, it can be seen that the 75% w/w conversion achieved without added product continually decreased in proportion to the added concentration of vanillylamine. Using MBA as amino donor, acetophenone will be liberated as the by-product of the reaction in stoichiometric amounts. As shown in Figure 7, without acetophenone addition a 92% w/w conversion could be achieved, but this fell to 77% w/w once added concentrations of acetophenone were above 10 mM. Concomitant reductions in initial reaction rate with increasing starting concentrations of acetophenone were also seen.

3.3.2 Determination of kinetic parameters

At this stage it would be desirable to develop a reliable enzyme kinetic model in order to predict reaction rate and yield over a range of bioreactor operating conditions. It is known that TAm requires the cofactor pyridoxal 5´-phosphate and that it catalyses enzymatic amino group transfer by a ping-pong bi–bi mechanism [40]. It has been reported for other TAm bioconversions that a substrate or product can bind to the enzyme, creating dead end complexes that cannot react further, causing a potentially strong irreversible inhibition [41, 42]. For the CV2025 TAm mediated synthesis of vanillylamine, the presence of abortive complexes in the reaction mechanism was not previously been determined; hence it was necessary to first elucidate the appropriate reaction mechanism.

The establishment of full kinetic models can be time and resource intensive, especially when using traditional linear data fitting methods [43]. We have recently published a nonlinear regression method to rapidly determine the best fitting reaction model and the values of the associated kinetic parameters [39]. Using this methodology, different kinetic models were initially fitted to the experimental initial rate data of Figures 4 and 5 to identify a solution in the vicinity of the global minimum for the Michaelis-Menten values of the forward reaction. Those values were

then used as initial guesses to perform non linear regressions of the data from Figures 6 and 7 to identify the exact location of the solution as well as the value of the other kinetic parameters. The initial value of k_r was set as $k_f/10$, since high equilibrium conversions were found experimentally, and the remainder of the initial values for the other constants were set to 1. Among all the models tested, the reaction mechanism shown in Figure 2 (B) which did not include any dead end complex formation gave the best statistical fit to the data [39].

The resulting kinetic model can be represented by Equation 1:

$$v = \left\{ k_f k_r E_{iTAm} \left([MBA][VAN] - \frac{[AP][VANAM]}{K_{eq}} \right) \right\} / den \qquad \text{Equation 1}$$

$$den = k_r K_{MBA}[VAN] + k_r K_{VAN}[MBA] + k_r[VAN][MBA] + \frac{k_f K_{AP}[VANAM]}{K_{eq}} + \frac{k_f K_{VANAM}[AP]}{K_{eq}} + \frac{k_f[AP][VANAM]}{K_{eq}} + \frac{k_r K_{MBA}[VAN][VANAM]}{K_{iVANAM}} + \frac{k_f K_{VANAM}[MBA][AP]}{K_{eq} K_{iMBA}}$$

where v represents the reaction rate, k_f and k_r represents the catalytic rate constants for the forward and reverse reaction respectively, K_{VAN}, K_{AP}, K_{VANAM} and K_{MBA} are the Michaelis constants of VAN (vanillin), AP (acetophenone), VANAM (vanillylamine) and MBA respectively, K_{iVANAM} and K_{iMBA} are the inhibition constants of VANAM and MBA respectively, K_{iMBA}, E_{iTAm} represents the TAm concentration and K_{eq} is the overall equilibrium constant. The values of the determined kinetic parameters are shown in Table II. Using these values, Figure 8 shows that good agreement was found between all the predicted and experimental data.

The kinetic constants of the CV2025 TAm using erythrulose (ERY) and MBA as substrates have already been published [39]. In that work a low Michaelis-Menten constant of MBA was also found, and the forward kinetic constant was 60% lower

than the one determined for vanillin in this work. The main kinetic bottleneck of the ERY and MBA TAm bioconversion was the high Michaelis-Menten constant of the amino acceptor ERY (95 mM). This bottleneck was alleviated in this work due to the 10 fold decrease in the Michaelis-Menten constant of the amino acceptor (8.5 mM), making vanillin a very suitable substrate for the CV2025 TAm.

The values of the kinetic parameters show that vanillylamine becomes inhibitory at concentrations that would limit the economic viability of the reaction. This limitation could be alleviated by the implementation of techniques such as *in situ* product removal [44]. Likewise inhibition by vanillin was also observed but was less severe than with the products. This limitation could be overcome via *in situ* substrate supply [45] or adoption of a fed-batch operating strategy (see Section 3.5).

3.4 **EVALUATION OF DIFFERENT BIOCATALYST FORMS**

For industrial implementation, it can be advantageous to select between one of either whole cell or isolated enzyme forms [46]. Consequently the activity and stability of both lysate and whole cell forms of the biocatalyst were evaluated.

Table III illustrates that both lysate and whole cell forms of the CV2025 ω-TAm biocatalyst could satisfactorily perform the bioconversion. Over 99% w/w conversion could be gained within 60 min when using the ω-TAm lysate while a minimum 88% w/w conversion was obtained using the whole cell form within the same time period. The initial rate of vanillylamine production from whole cell form is calculated as 0.12 $mM.min^{-1}$ which is 0.1 $mM.min^{-1}$ less than that from lysate form. In addition, the half-life of both biocatalyst forms was also examined with regard to longer term operational stability. The results in Table III indicate that both ω-TAm biocatalyst forms were stable over 24 hr. These results indicate both biocatalyst forms are suitable for vanillin bioconversion.

3.5 FED-BATCH VANILLIN BIOCONVERSIONS

In order to overcome the substrate inhibition effects seen in Section 3.3.1, fed-batch bioconversion operation was investigated [47]. Various feeding strategies were investigated and enabled increased final product concentrations to be obtained as shown in Figure 9. Figure 9 (A) shows results for fed-batch reactions, involving low initial substrate concentrations (5 mM vanillin, 10 mM MBA) and low feed concentrations (5 mM vanillin, 10 mM MBA). This demonstrates virtually quantitative vanillin utilization over 3 consecutive feed additions and concomitant increases in vanillylamine production. Overall the product concentration obtained was 2.7 $g.L^{-1}$ (14.2 mM) and greater than 88% w/w substrate conversion was achieved. Results for fed-batch reactions carried out at higher substrate concentrations and high feed concentrations are shown in Figure 9 (B). This shows further increases in product concentration up to 5.5 $g.L^{-1}$ (35.9 mM). However there was only 30% w/w vanillin conversion after the first batch. The residual vanillin concentration then increased following each feed addition leading to a poor overall conversion of just 8% w/w.

These results suggest that fed-batch operation would be a valuable strategy to adopt at larger scales. A practical limitation encountered was the limited solubility of vanillin in the aqueous feed solutions of up to 65 mM. This might necessitate use of a co-solvent, although this would be less environmentally acceptable. The issues of product inhibition would still need to be overcome as discussed in Section 3.3.2.

4. CONCLUSIONS

This work demonstrates that the CV2025 ω-TAm is a useful biocatalyst for conversion of lignin breakdown products arising from either thermochemical pre-treatment or biodegradation processes. A range of breakdown products could be converted using (S)-α-methylbenzylamine as amine donor with the best being vanillin. At low substrate concentrations, the bioconversion of vanillin to vanillylamine displayed high reaction rates and yields. However, the rates and yields of the

bioconversion decreased at higher concentrations due to both substrate and product inhibition. Using a fed-batch operating strategy product concentrations up to 5.5 $g.L^{-1}$ could be achieved but at the expense of substrate conversion. Further increases in the space-time yield of the bioconversion would be necessary for this process to become economically viable. Both *in situ* product removal and directed enzyme evolution strategies [48] are currently being investigated in our laboratory.

Acknowledgements

C.J. Du would like to thank the UCL Department of Biochemical Engineering for providing financial support from the Peter Dunnill scholarship fund.

5. REFERENCES

1. Saha BC, Demirjian DC, American Chemical Society M, Advances in applied b, American Chemical Society. Division of Biochemical T, American Chemical S (2001) Applied biocatalysis in specialty chemicals and pharmaceuticals, Oxford : American Chemical Society ; Oxford University Press [distributor], Washington, D.C.

2. Pollard DJ, Woodley JM (2007) Biocatalysis for pharmaceutical intermediates: the future is now. Trends Biotechnol 25:66-73.

3. Prather KL, Martin CH (2008) *De novo* biosynthetic pathways: rational design of microbial chemical factories. Curr Opin Biotechnol 19:468-74.

4. Huisman GW, Collier SJ (2013) On the development of new biocatalytic processes for practical pharmaceutical synthesis. Curr Opin Chem Biol 17:284-92.

5. Henderson RK, Jimenez-Gonzalez C, Preston C, Constable DJC, Woodley JM (2008) EHS & LCA assessment for 7-ACA synthesis: A case study for comparing biocatalytic & chemical synthesis. Ind Biotech 4:180-192.

6. Fan PH (2000) Price uncertainty and vertical integration: an examination of petrochemical firms. J Corp Finance 6:345-376.

7. Wang SY, Li D (2011) The Spillover Effects on Petrochemical industrial

concentration of International Oil Price. Energy Procedia 5:2444-2448.

8. Vicuna R (1988) Bacterial degradation of lignin. Enzyme Microb Technol 10:646-655.

9. Bonini C, D' Auria M, Maggio PD, Ferri R (2008) Characterization and degradation of lignin from steam explosion of pine and corn stalk of lignin: The role of superoxide ion and ozone. Ind Crops Prod 27:182-188.

10. Mohtashamipur E, Norpoth K (1990) Release of mutagens after chemical or microbial degradation of beech wood lignin. Toxicol Lett 51:277-85.

11. Zimmermann W (1990) Degradation of lignin by bacteria. J Biotechnol 13:119-130.

12. Fiechter A (1993) Function and synthesis of enzymes involved in lignin degradation. J Biotechnol 30:49-55.

13. Bonini C, D' Auria M (2004) Degradation and recovery of fine chemicals through singlet oxygen treatment of lignin. Ind Crops Prod 20:243-259.

14. Bugg TD, Ahmad M, Hardiman EM, Rahmanpour R (2011) Pathways for degradation of lignin in bacteria and fungi. Nat Prod Rep 28:1883-96.

15. Crawford RL, Crawford DL (1984) Recent advances in studies of the mechanisms of microbial degradation of lignins. Enzyme Microb Technol 6:434-442.

16. Eriksson KE (1993) Concluding remarks: where do we stand and where are we going? Lignin biodegradation and practical utilization. J Biotechnol 30:149-58.

17. Tuomela M, Vikman M, Hatakka A, Itavaara M (2000) Biodegradation of lignin in a compost environment: a review. Bioresour Technol 72:169-183.

18. FitzPatrick M, Champagne P, Cunningham MF, Whitney RA (2010) A biorefinery processing perspective: treatment of lignocellulosic materials for the production of value-added products. Bioresour Technol 101:8915-22.

19. Azadi P, Inderwildi OR, Farnood R, King DA (2013) Liquid fuels, hydrogen and chemicals from lignin: A critical review. Renew Sust Energ Rev 21:506-523.

20. Taniguchi M, Suzuki H, Watanabe D, Sakai K, Hoshino K, Tanaka T (2005) Evaluation of pretreatment with Pleurotus ostreatus for enzymatic hydrolysis of rice straw. J Biosci Bioeng 100:637-43.

21. Huisman GW, Gray D (2002) Towards novel processes for the fine-chemical and pharmaceutical industries. Curr Opin Biotechnol 13:352-8.

22. Ralph NS, Cheol HY, Kyung WJ (2001) Synthesis of secondary amines. Tetrahedron 57:7785-7811.

23. Said SA (2002) Stereoselective Transformations of Chiral Amines. Department of Chemistry: Norwegian University of Science and Technology. pp. 1-26.

24. Sheldon RA (1996) Chirotechnology: Designing economic chiral syntheses. J Chem Tech Biotechnol 67:1-14.

25. Shin JS, Kim BG (1997) Kinetic resolution of alpha-methylbenzylamine with omicron-transaminase screened from soil microorganisms: application of a biphasic system to overcome product inhibition. Biotechnol Bioeng 55:348-58.

26. Shin JS, Kim BG, Liese A, Wandrey C (2001) Kinetic resolution of chiral amines with omega-transaminase using an enzyme-membrane reactor. Biotechnol Bioeng 73:179-87.

27. Kaulmann U, Smithies K, Smith MEB, Hailes HC, Ward JM (2007) Substrate spectrum of ω-transaminase from *Chromobacterrium violaceum* DSM30191 and its potential for biocatalysis. Enzyme Microb Technol 41:628-637.

28. Rudat J, Brucher BR, Syldatk C (2012) Transaminases for the synthesis of enantiopure beta-amino acids. AMB Express 2:11.

29. Schell U, Wohlgemuth R, Ward JM (2009) Synthesis of pyridoxamine 5'-phosphate using an MBA:pyruvate transaminase as biocatalyst. J Mol Catal B Enzym 59:279-285.

30. Bradford MM (1976) A rapid and sensitive method for the quantitation of microgram quantities of protein utilizing the principle of protein-dye binding. Anal Biochem 72:248-54.

31. King J, Laemmli UK (1971) Polypeptides of the tail fibres of bacteriophage T4. J Mol Biol 62:465-77.

32. Fahmi R, Bridgwater AV, Thain SC, Donnison IS, Morris PM, Yates N (2007) Prediction of Klason lignin and lignin thermal degradation products by Py-GC/MS in a collection of *Lolium* and *Festuca* grasses. J Anal Appl Pyrolysis 80:16-23.

33. Ko JJ, Shimizu Y, Ikeda K, Kim SK, Park CH, Matsui S (2009) Biodegradation of high molecular weight lignin under sulfate reducing conditions: lignin degradability and degradation by-products. Bioresour Technol 100:1622-7.

34. Werhan H, Farshori A, Von Rohr PR (2012) Separation of lignin oxidation products by organic solvent nanofiltration. J Membrane Sci 423-424:404-412.

35. Savile CK, Janey JM, Mundorff EC, Moore JC, Tam S, Jarvis WR, Colbeck JC, Krebber A, Fleitz FJ, Brands J, Devine PN, Huisman GW, Hughes GJ (2010) Biocatalytic asymmetric synthesis of chiral amines from ketones applied to sitagliptin manufacture. Science 329:305-9.

36. Meyer O, Heddesheimer I (2005) Process for preparing vanillylamine hydrochloride. U.S: Boehringer Ingelheim Pharma KG, Ingelheim (DE). pp. 3.

37. Borregaard (2011) Climate friendly products. Available at: http://www.borregaard.com/content/view/full/10191/(language)/eng-GB. Accessed on 11.Oct.2011.

38. Yi SS, Lee CW, Kim J, Kyung D, Kim BG, Lee YS (2007) Covalent immobilization of ω-transaminase from *Vibrio fluvialis* JS17 on chitosan beads. Process Biochem 42:895-898.

39. Rios-Solis L, Bayir N, Halim M, Du C, Ward JM, Baganz F, Lye GJ (2013) Non-linear kinetic modelling of reversible bioconversions: Application to the transaminase catalyzed synthesis of chiral amino-alcohols. Biochem Eng J 73:38-48.

40. Kuramitsu S, Hiromi K, Hayashi H, Morino Y, Kagamiyama H (1990) Pre-steady-state kinetics of Escherichia coli aspartate aminotransferase catalyzed reactions and thermodynamic aspects of its substrate specificity. Biochemistry 29:5469-76.

41. Shin JS, Kim BG (1998) Kinetic modeling of omega-transamination for enzymatic kinetic resolution of alpha-methylbenzylamine. Biotechnol Bioeng 60:534-40.

42. Shin JS, Kim BG (2002) Exploring the active site of amine:pyruvate aminotransferase on the basis of the substrate structure-reactivity relationship: how the enzyme controls substrate specificity and stereoselectivity. J Org Chem 67:2848-53.

43. Chen BH, Hibbert EG, Dalby PA, Woodley JM (2008) A new approach to bioconversion reaction kinetic parameter identification. Am Inst Chem Eng J

54:2155-2163.

44. Lye GJ, Woodley JM (1999) Application of in situ product-removal techniques to biocatalytic processes. Trends Biotechnol 17:395-402.

45. Schmolzer K, Madje K, Nidetzky B, Kratzer R (2012) Bioprocess design guided by in situ substrate supply and product removal: process intensification for synthesis of (S)-1-(2-chlorophenyl)ethanol. Bioresour Technol 108:216-23.

46. Duetz WA, Beilen JBV, Witholt B (2001) Using proteins in their natural environment: potential and limitations of microbial whole-cell hydroxylations in applied biocatalysis. Curr Opin Biotechnol 12:419-425.

47. Ko CL, Wang FS (2006) Run-to-run fed-batch optimization for protein production using recombinant *Escherichia coli*. Biochem Eng J 30:279-285.

48. Hibbert EG, Baganz F, Hailes HC, Ward JM, Lye GJ, Woodley JM, Dalby PA (2005) Directed evolution of biocatalytic processes. Biomol Eng 22:11-9.

List of Tables

Table I

Lignin Breakdown Intermediate	Structure	Activity Detected
Vanillin	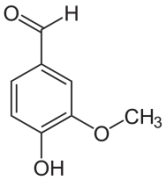	✓
Coniferyl aldehyde	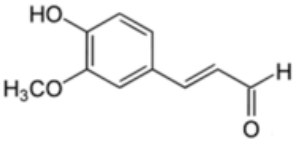	✓
Trans-cinnamaldehyde	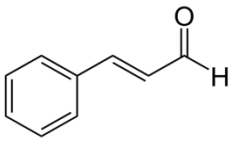	✓
Benzaldehyde	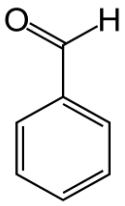	✓
p-hydroxyacetophenone	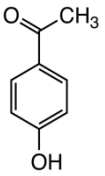	✓
Acetovanillone	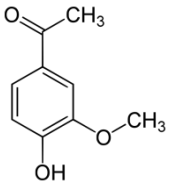	✓
Caffeic acid	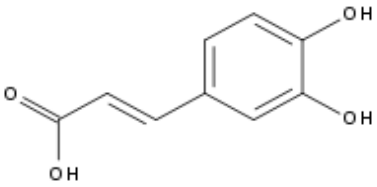	✗
Ferulic acid	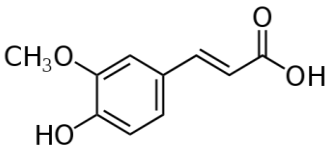	✗

Table II

Kinetic parameter	**Reconciled value**
Rate constant forward reaction (s^{-1}): k_f	2.6
Rate constant reverse reaction (s^{-1}): k_r	0.28
Michaelis constant for MBA (mM): K_{MBA}	1.3×10^{-2}
Michaelis constant for VAN (mM): K_{VAN}	8.54
Michaelis constant for AP (mM): K_{AP}	7.6×10^{-2}
Michaelis constant for VANAM(mM): K_{VANAM}	5.3×10^{-2}
Inhibition constant for MBA (mM): K_{iMBA}	6.9
Inhibition constant for VAN (mM): K_{iVAN}	3.3×10^{-3}
Inhibition constant for AP (mM): K_{iAP}	378
Inhibition constant for VANAM (mM): K_{iVANAM}	2.0×10^{-4}
Global equilibrium constant: K_{eq}	3.3

Table III

Hold Time (hr)	Lysate			Whole Cell		
	Initial rate of vanillin utilisation ($mM.min^{-1}$)	Initial rate of vanillylamine production ($mM.min^{-1}$)	Vanillylamine yield (% w/w)	Initial rate of vanillin utilisation ($mM.min^{-1}$)	Initial rate of vanillylamine production ($mM.min^{-1}$)	Vanillylamine yield (% w/w)
0	0.29	0.22	99	0.17	0.14	93
2	0.29	0.21	99	0.16	0.12	90
4	0.29	0.21	99	0.13	0.11	88
6	0.29	0.23	99	0.15	0.11	89
8	0.29	0.22	99	0.16	0.12	89
24	0.29	0.22	99	0.15	0.13	89

List of Figure Legends

Figure 1. Shake flask culture of *E. coli* BL21 (DE3) Gold expressing CV2025 ω-TAm from the plasmid pQR801: (A) growth kinetics for induced (with 0.1 mM IPTG) (▲) and non-induced cells (◆); (B) analysis of over-expression of the 47 kDa ω-TAm. SDS PAGE analysis shows molecular weight markers (Lane 1), induced (Lanes 2-3) and non-induced (Lanes 4-5) cells. Shake flask cultures performed as described in Section 2.3 and SDS-PAGE performed as described in Section 2.5.3.

Figure 2. Proposed reaction mechanism for the ω-TAm mediated synthesis of vanillylamine using MBA as amino donor. VAN (vanillin), VANAM (vanillylamine), AP (acetophenone), E-PLP (enzyme bound pyridoxal 5'-phosphate), E-PMP (enzyme bound pyridoxamine 5'-phosphate).

Figure 3. Confirmation of vanillin bioconversion by CV2025 ω-TAm lysate: vanillin consumption (▲), vanillylamine production (■). Experimental conditions: pH 7.5, 30^{o}C, 350 rpm, 300 μL, [vanillin] = 20 mM, [MBA] = 20 mM, 50 mM Tris buffer, 0.2 mM PLP. Experiments performed as described in Section 2.4.1.

Figure 4. Effect of initial vanillin concentration on bioconversion kinetics using CV2025 ω-TAm lysate: (A) vanillin utilization; (B) vanillylamine production. Experimental conditions: pH 7.5, 30^{o}C, 350 rpm, 300 μL, [vanillin] = 5 mM (◆), 10 mM (□), 20 mM (▲) and 25 mM （○）, [MBA] = 30 mM, 50 mM Tris buffer, 0.2 mM PLP. Experiments performed as described in Section 2.4.3. Error bars indicate the mean (n=3), ± one standard deviation.

Figure 5. Effect of initial MBA concentration on bioconversion kinetics using CV2025 ω-TAm lysate: (A) vanillin utilization; (B) vanillylamine production. Experimental conditions: pH 7.5, 30^{o}C, 350 rpm, 300 μL, [MBA] = 5 mM (■), 10 mM (□), 20 mM (▲), 30 mM (△), 40 mM (●) and 50 mM (○), [vanillin] = 5 mM, 50 mM Tris buffer, 0.2 mM PLP. Experiments performed as described in Section 2.4.3. Error bars indicate the mean (n=3), ± one standard deviation.

Figure 6. Effect of added vanillylamine on the bioconversion kinetics of CV2025 ω-TAm lysate: (A) vanillin utilization; (B) vanillylamine production with different initial added concentrations of vanillylamine: 0 mM (■), 5 mM (□), 10 mM (▲), 20 mM (△). Experimental conditions: pH 7.5, 30^{o}C, 350 rpm, 300 μL, [MBA] = 40 mM, [vanillin] = 20 mM, 50 mM Tris buffer, 0.2 mM PLP. Experiments performed as described in Section 2.4.3. Error bars indicate the mean (n=3), ± one standard deviation.

Figure 7. Effect of added acetophenone on the bioconversion kinetics of CV2025 ω-TAm lysate: (A) vanillin utilization; (B) vanillylamine production with different

initial added concentrations of acetophenone: 0 mM (●), 5 mM (■), 10 mM (▲). Experimental conditions: pH 7.5, 30°C, 350 rpm, 300 μL, [MBA] = 10 mM, [vanillin] = 10 mM, 50 mM Tris buffer, 0.2 mM PLP. Experiments performed as described in Section 2.4.3. Error bars indicate the mean (n=3), ± one standard deviation.

Figure 8. Comparison of experimental data of vanillin (◆), MBA (■), vanillylamine (▲) and model predictions (solid lines). Experimental conditions: pH 7.5, 30°C, 350 rpm, 300 μL, [MBA] = 40 mM, [vanillin] = 20 mM, 50 mM Tris buffer, 0.2 mM PLP. Experimental data gained from Figure 4, 5, 6 and 7. Model predictions calculated from Equation 1 using kinetic parameters from Table II.

Figure 9. Fed-batch vanillin bioconversion kinetics using CV2025 ω-TAm in lysate form: vanillin utilization (■), vanillylamine production (▲). (A) Low substrate concentrations: [MBA] = 10 mM, [vanillin] = 5 mM. (B) High substrate concentrations: [MBA] = 60 mM, [vanillin] = 40 mM. Experimental conditions: pH 7.5, 30°C, 350 rpm, 15 mL, 50 mM Tris buffer, 0.2 mM PLP. Experiments performed as described in Section 2.4.6.

Figure 1

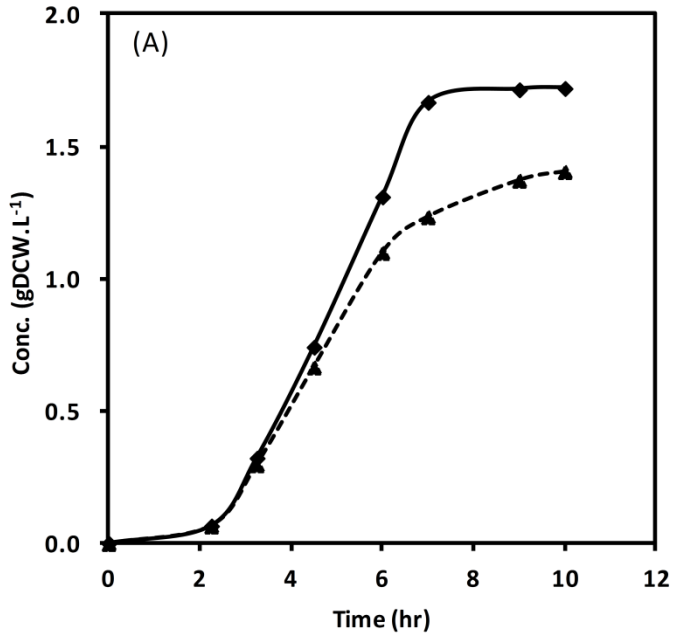
(A)
2.0
1.5
1.0
0.5
0.0
Conc. (gDCW.L-1)
0
2
4
6
8
10
12
Time (hr)

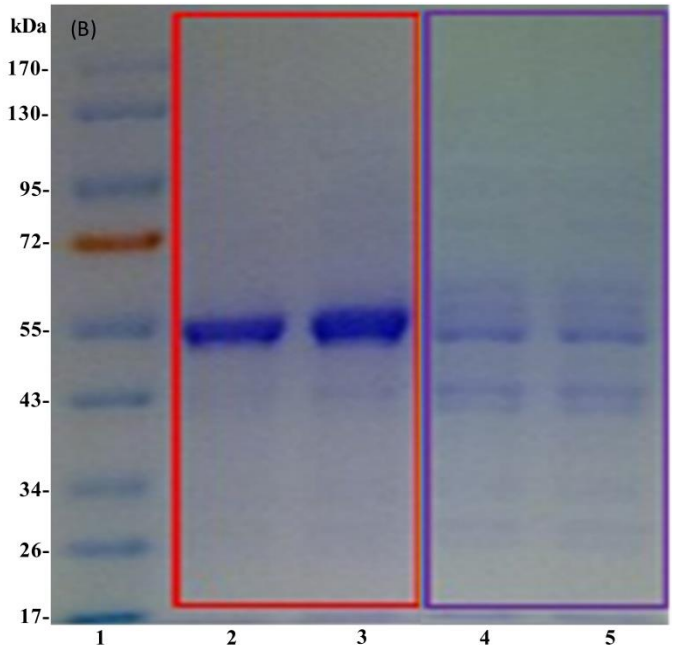
kDa
(B)
170-
130-
95-
72-
55-
43-
34-
26-
17-
1
2
3
4
5

Figure 2

A) Overall reaction

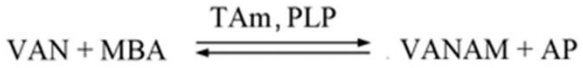

B)Reaction scheme

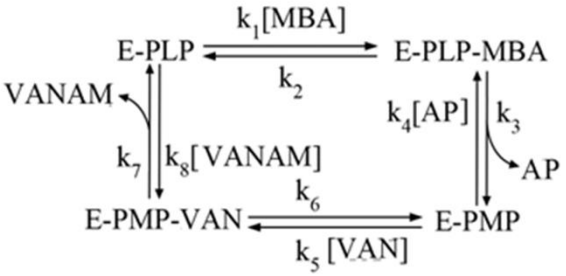

Figure 3

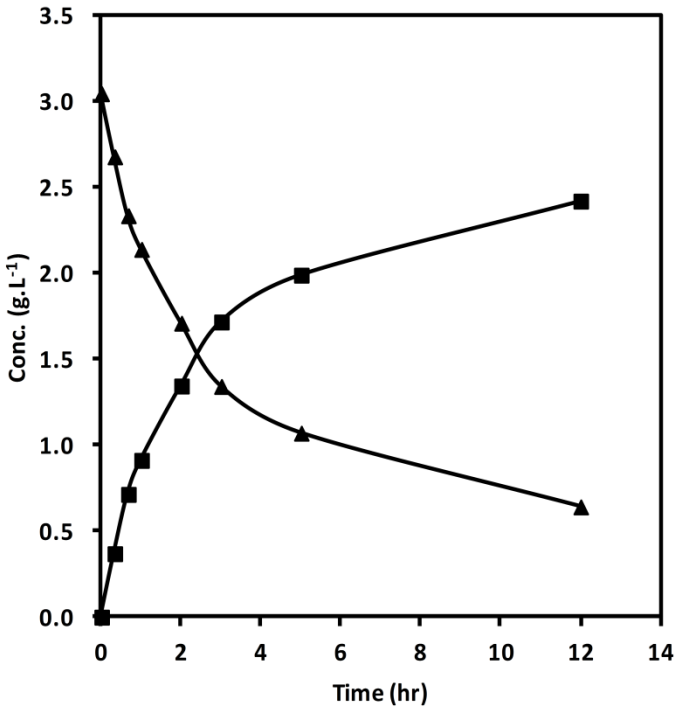

Figure 4

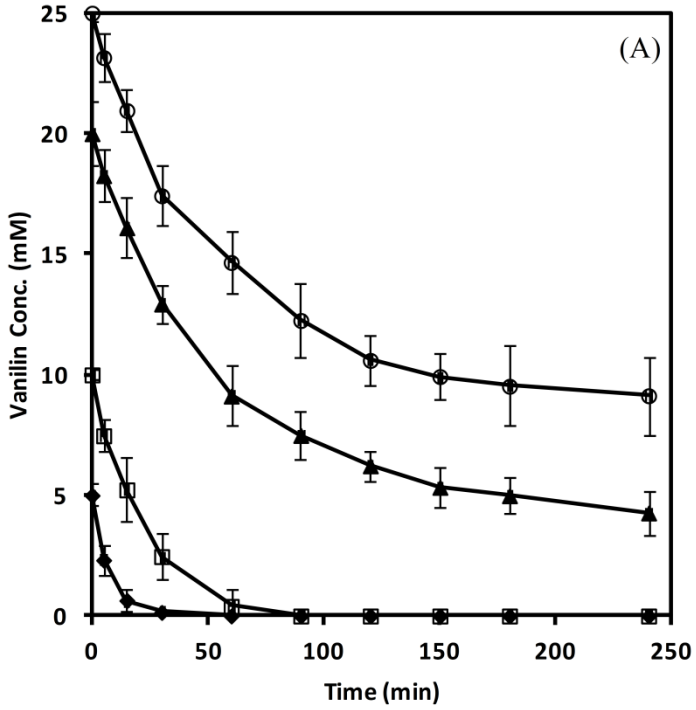
(A)
Vanilin Conc. (mM)
Time (min)
0
5
10
15
20
25
0
50
100
150
200
250

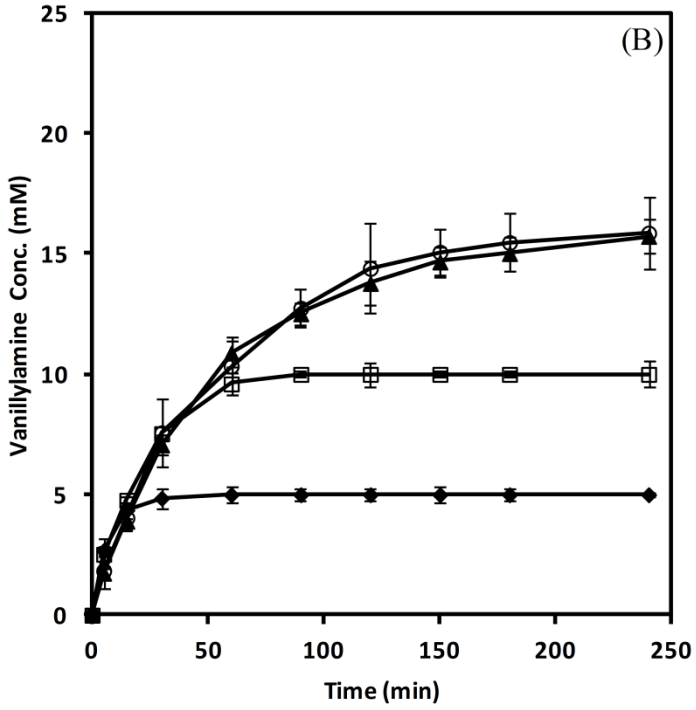
(B)
Vanillylamine Conc. (mM)
Time (min)
0
5
10
15
20
25
0
50
100
150
200
250

Figure 5

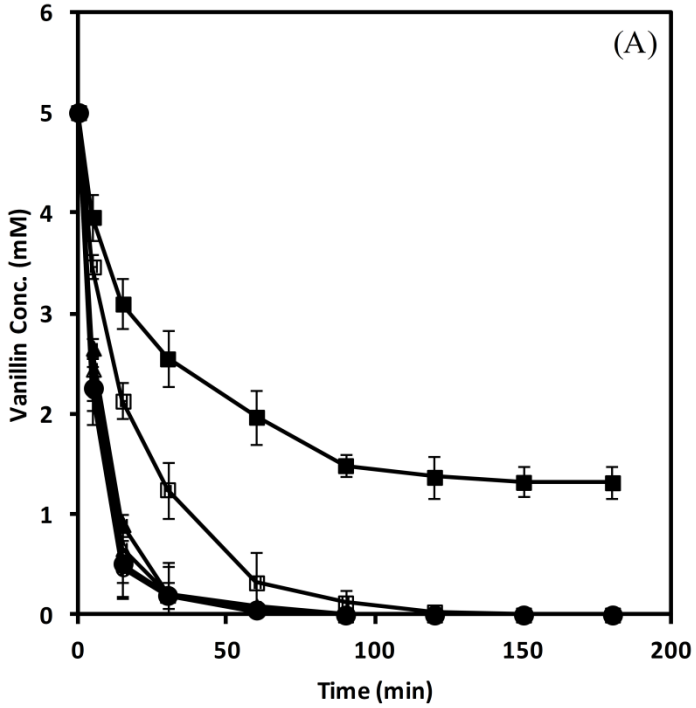
(A)
Vanillin Conc. (mM)
Time (min)
0
1
2
3
4
5
6
0
50
100
150
200

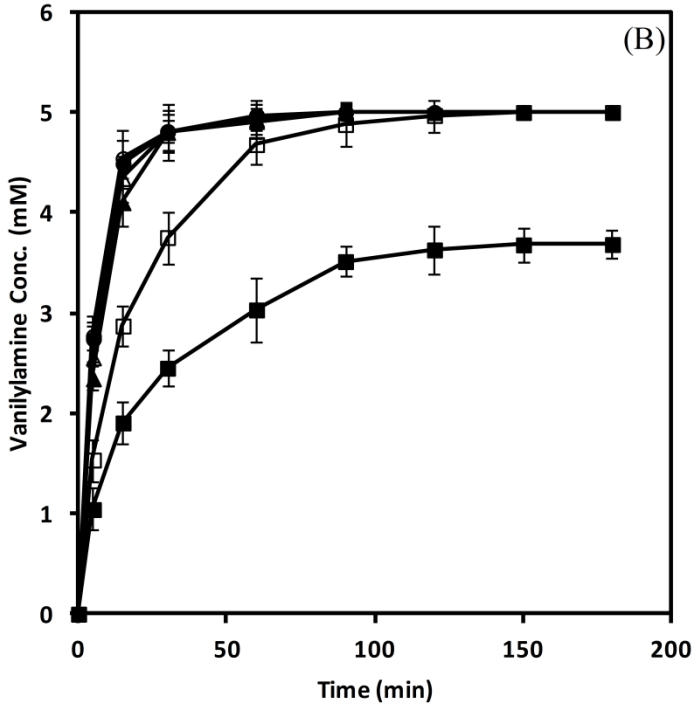
(B)
Vanilylamine Conc. (mM)
Time (min)
0
1
2
3
4
5
6
0
50
100
150
200

Figure 6

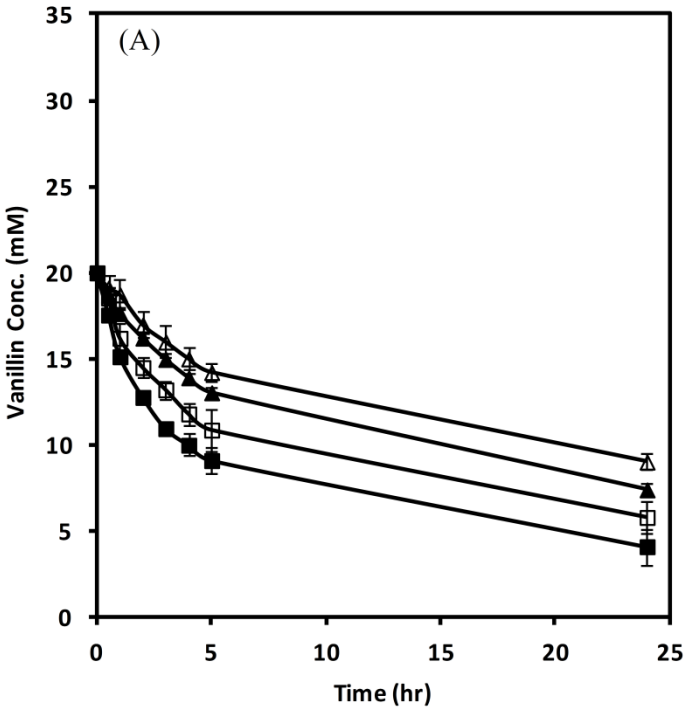
(A)
Vanillin Conc. (mM)
Time (hr)
0
5
10
15
20
25
30
35

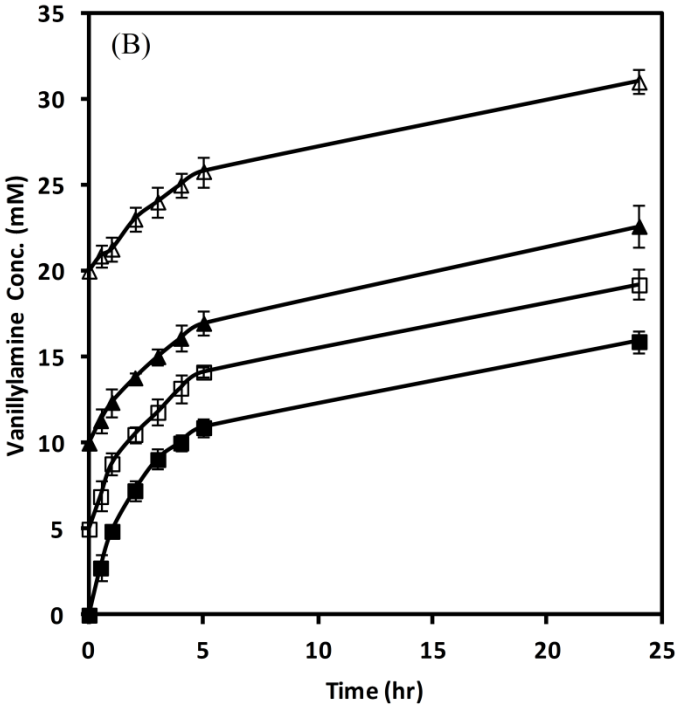
(B)
Vanillylamine Conc. (mM)
Time (hr)
0
5
10
15
20
25
30
35

Figure 7

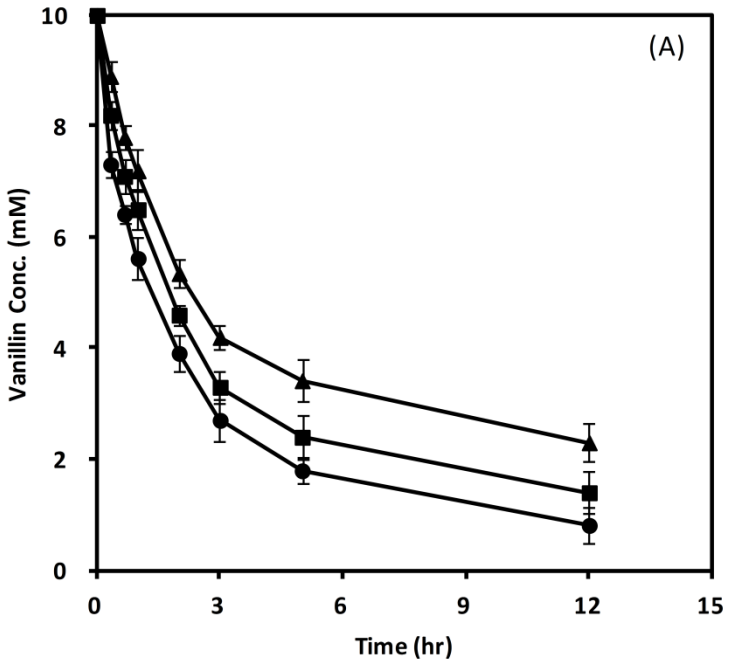
(A)
Vanillin Conc. (mM)
Time (hr)
0
2
4
6
8
10
0
3
6
9
12
15

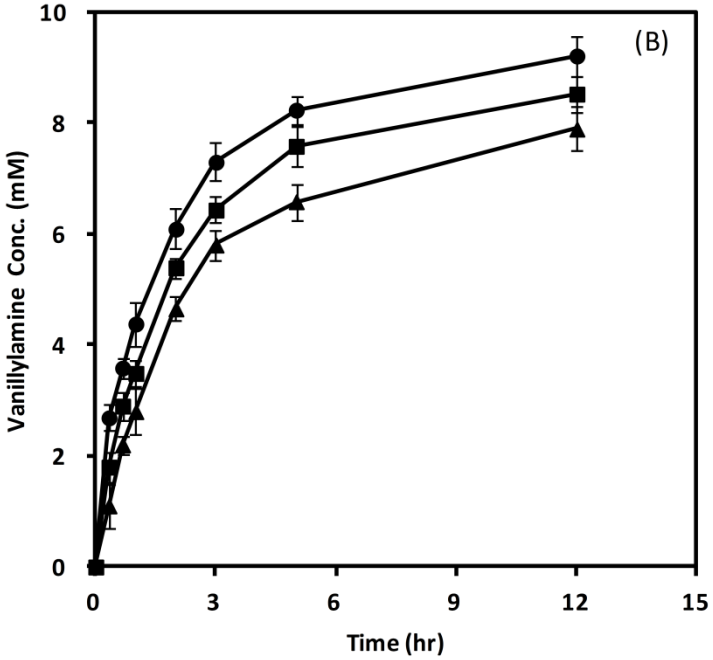
(B)
Vanillylamine Conc. (mM)
Time (hr)
0
2
4
6
8
10
0
3
6
9
12
15

Figure 8

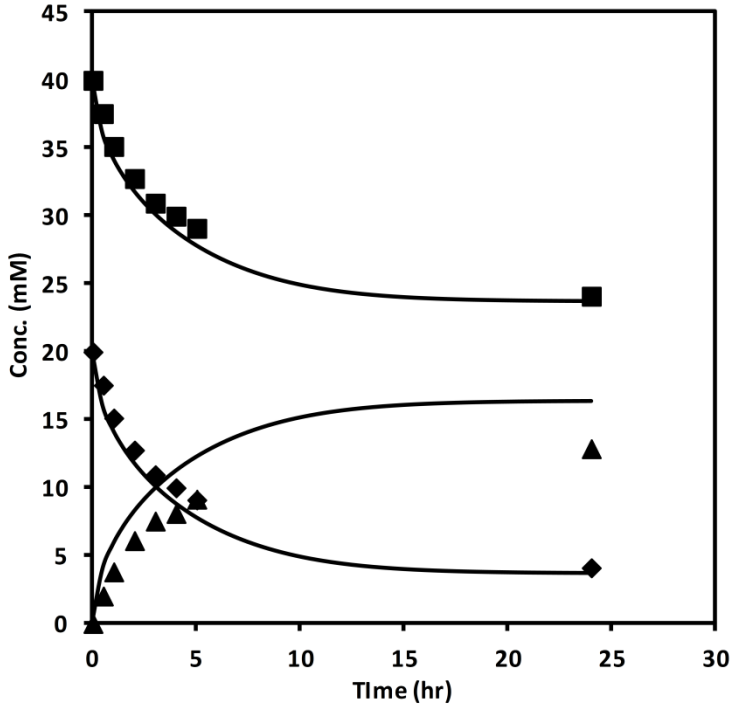

Figure 9

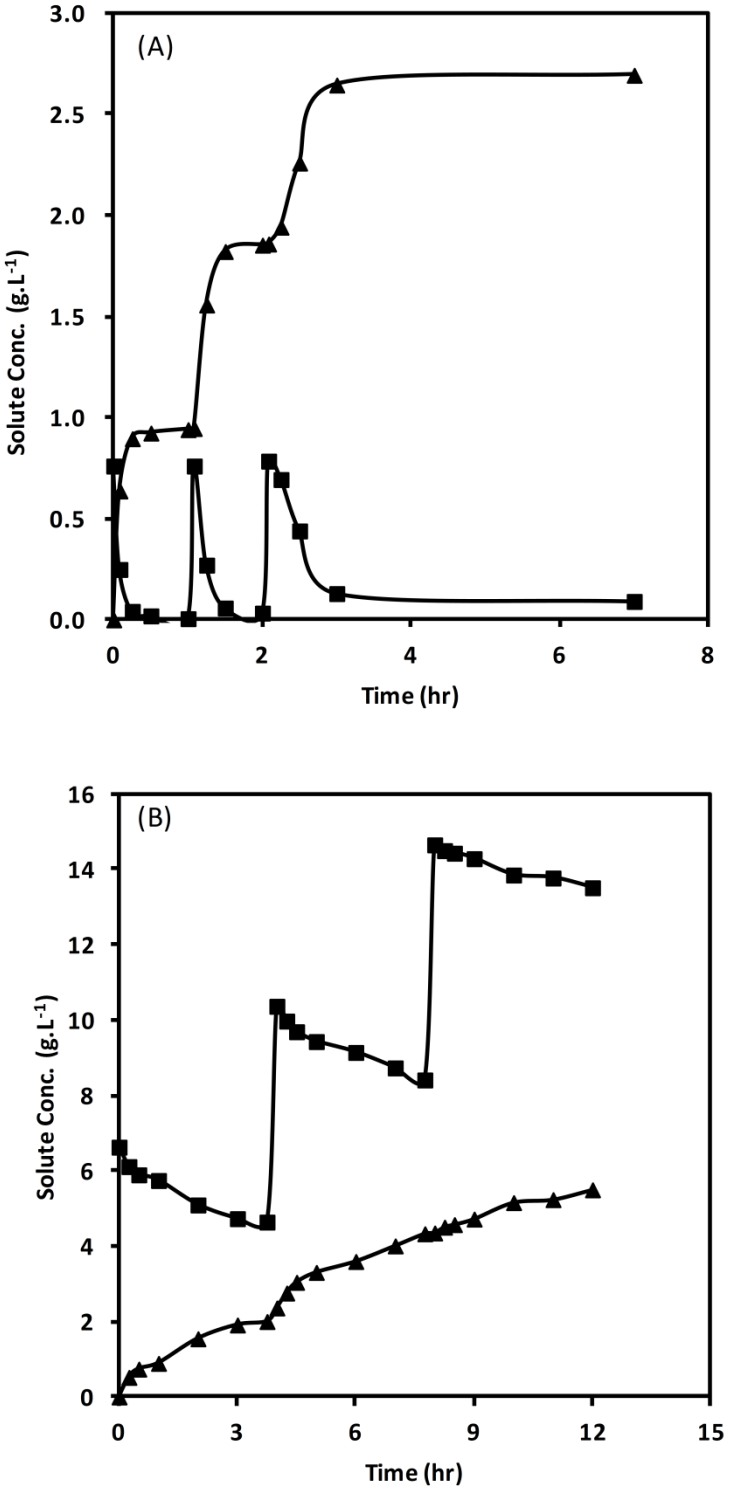
(A)
Solute Conc. (g.L-1)
Time (hr)
0.0
0.5
1.0
1.5
2.0
2.5
3.0
0
2
4
6
8
(B)
Solute Conc. (g.L-1)
Time (hr)
0
2
4
6
8
10
12
14
16
0
3
6
9
12
15

ADDITIONAL INFORMATION

Mass Spectrometry Confirmation of product vanillylamine by Mass Spectrometry.

NMR Confirmation of product vanillylamine by NMR.

Mass Spectrometry Spectrum obtained from bioconversion shown in Figure 3 for sample taken at 12 hr.

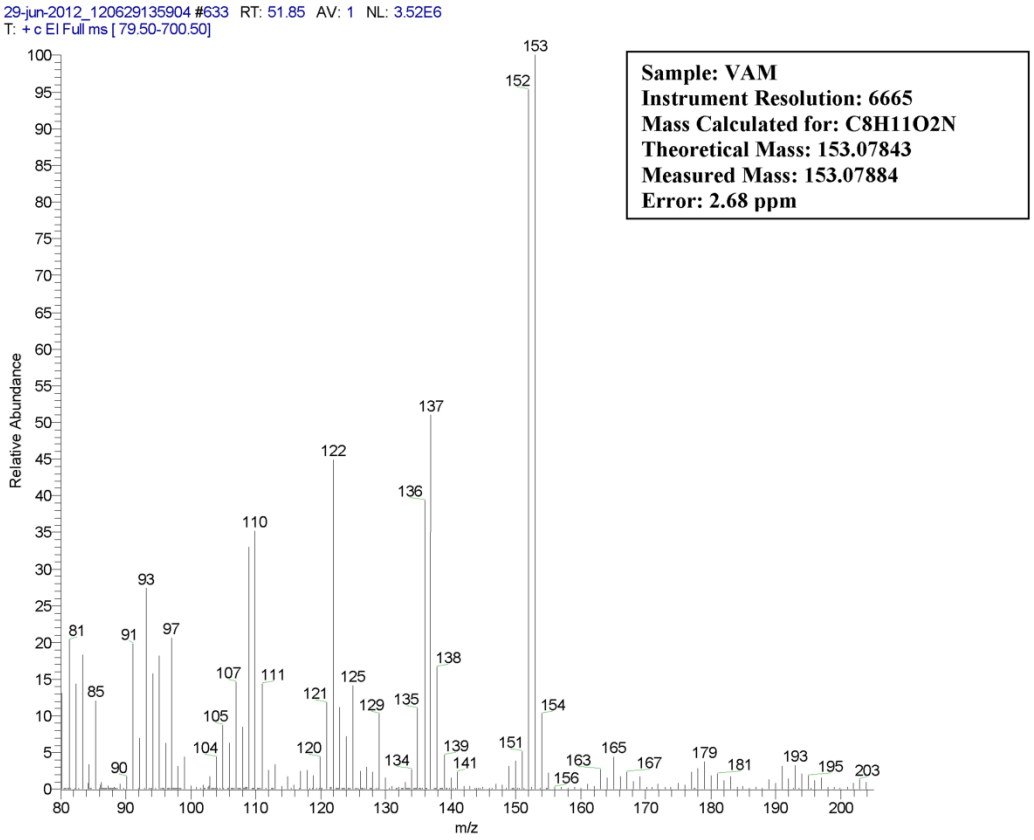

The mass-to-charge ratio (m/Q) expected of vanillylamine was 153.07843, which was confirmed by mass spectrometry obtaining a result of 153.07884 (error of 2.68 ppm).

NMR Spectrum obtained from bioconversion shown in Figure 3 for sample taken at 12 hr.

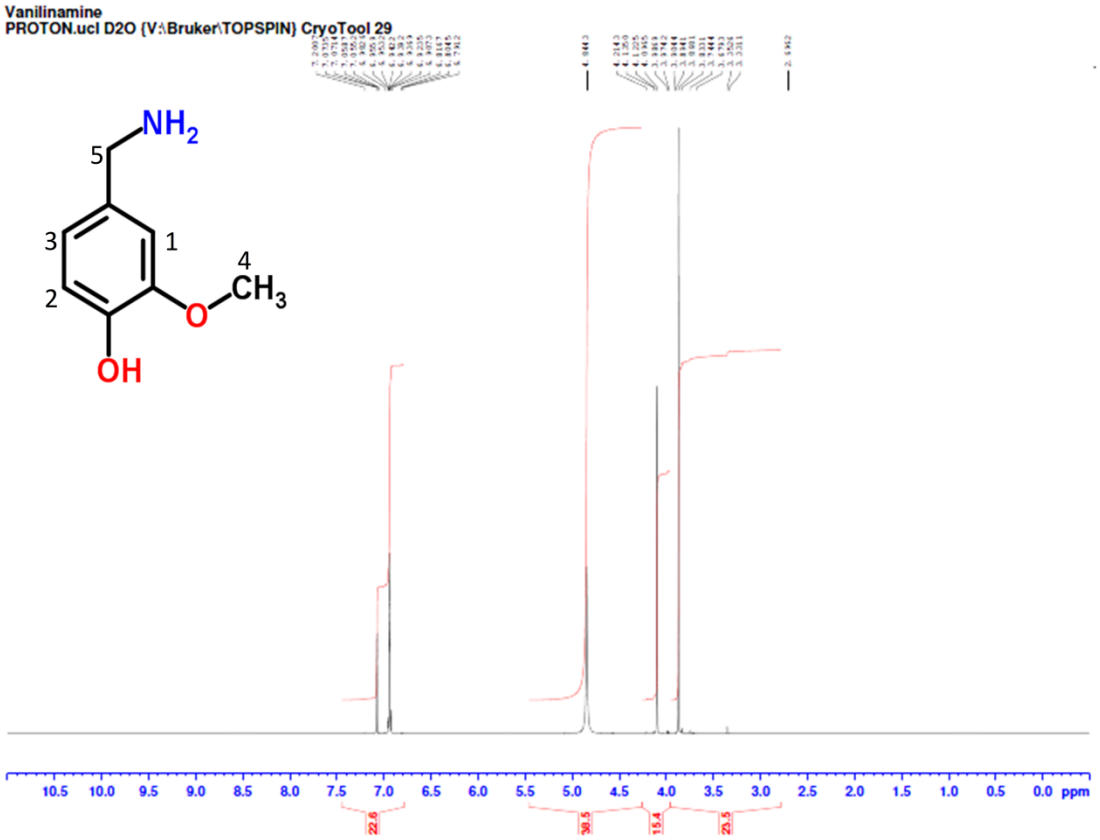

NMR results displayed the characteristic spectrum peaks at 7.08 ppm for the aromatic hydrogen in carbon 1 and at 6.93 ppm for hydrogens in carbon 2 and 3, which the ratio of integrated area was expected to be 2:1 compared to the hydrogen of carbon 1 (1.984 vs 1.000). The signal of the hydrogen of carbon 4 is shown at 3.87 ppm, with 3 times the area intensity compared to the hydrogen in carbon 1 as expected (3.0255 vs 1.000). The previously mentioned signals would have been expected to be obtained from a sample of both vanillin and vanillylamine. The signal for the two vanillylamine hydrogens in carbon 5 can be observed at 4.1 ppm, and it presented a ratio of integrated area of 2:1 in comparison to the hydrogen in carbon 1 as expected. This was a clear result to differentiate the sample from vanillin, from which the ratio of integrated area would had been expected to be 1:1 in comparison to carbon 1, because vanillin has only 1 hydrogen in carbon 5. Also no signal of the aldehyde group of vanillin was detected in the expected region of 8-10 ppm.